Supporting Information for:

Two-photon excitable membrane targeting polyphenolic carbon dots for long-term imaging and pH-responsive chemotherapeutic drug delivery for synergistic tumor therapy

Sayan Deb Dutta,[1+] Jin Hexiu,[2+] Jongsung Kim,[3] Sourav Sarkar,[4] Jagannath Mondal,[5], Jeong Man An,[6] Yong-Kyu Lee,[5] Md Moniruzzaman,[3*] and Ki-Taek Lim[1*]

[1]*Department of Biosystems Engineering, College of Agriculture and Life Sciences, Kangwon National University, Chuncheon-24341, Republic of Korea.*
[2]*Department of Plastic and Traumatic Surgery, Capital Medical University, Beijing-100069, Fengtai, China.*
[3]*Department of Chemical and Biological Engineering, Gachon University, Seongnam-1342, Republic of Korea.*
[4]*Department of Chemistry, Pohang University of Science and Technology, Pohang, Gyungbuk-37673, Republic of Korea.*
[5]*Department of Green Bioengineering, Korea National University of Transportation, Chungju-27470, Republic of Korea.*
[6]*Department of Bioengineering, College of Engineering, Hanyang University, Seoul-04763, Republic of Korea.*

[*]**Corresponding Author(s):** mani57chem@gachon.ac.kr and ktlim@kangwon.ac.kr

Experimental Sections

CQDs synthesis and characterization

Synthesis of green-emissive CQDs (g-CQDs)

The *g*-CQDs was synthesized as reported elsewhere with slight modification [1, 2]. In a typical synthesis, 200 mg phloroglucinol (Sigma-Aldrich, USA) was dispersed in 2 mL DW. After that, 2 mL of concentrated H_2SO_4 was added to the mixture. After stirring for 15 min, the pale yellowish solution was kept in a hot air preheated at 190 °C for 56 min to obtain the *g*-CQDs. The solution was cooled at ambient temperature and 5 mL DW was added in the resulting mixture, followed by centrifugation at 13,000 rpm for 10 min. The obtained black mass was rinsed with deionized water several times and dialyzed using a cellulose membrane (MW cut-off 100-500 Da) for 48 h. The dialyzed product was dried at 60 °C, dispersed in pure ethanol, and centrifuged at 6000 rpm for 5 min to discard agglomerated particles. Finally, the dried powder was stored in ambient temperature.

Characterization of g-CQDs

The high-resolution TEM (JEM 3010, Jeol, Japan) was used to observe the structure of the *g*-CQDs. The optical properties of the CQDs was monitored using UV-Vis spectrophotometer (Softmax Pro Molecular Device, California, USA), and PL spectrometer (Quanta Master, New Jersey, USA), respectively. The surface potential (ζ-potential) was measured by using a particle size analyzer (Malvern PANalytical, Netherlands, UK). The Fourier-transform infrared (FT-IR) spectra was recorded using a FT-IR spectrometer (Bruker Vortex 70, Massachusetts, USA). The surface functional group was monitored by X-ray photoelectron spectroscopy (XPS, Thermo Scientific, USA) using an X-ray source with twin-anode gun (Al-Kα+, hν = 1486.6 eV) and a monochromatic gun. The crystallinity of the CQDs was measured using an X-ray diffractometer

(PANalytical, Netherlands, UK) with a 3 kW X-ray generator and 2.2 kW ceramic X-ray tube. The Raman spectrometer (Horiba Jobin, ARAMIS, New Jersey, USA) was used to record the Raman spectra of the CQDs, respectively.

Quantum yield measurement

The quantum yield of the as-prepared *g*-CQDs was measured using quinine sulfate (QY: 54% in 0.1 M H_2SO_4) as a reference value. All the absorbance value of *g*-CQDs were kept under 0.1 to avoid reabsorption, and the PL spectra was recorded at the excitation of 350 nm. The integrated fluorescence intensity (IFI) was calculated by measuring the area under the PL curve. Finally, the QY of the *g*-CQDs was calculated using following equation:

$$\Phi_x = \Phi_{st}\left(\frac{I_x}{I_{st}}\right)\left(\frac{{\eta_x}^2}{{\eta_{st}}^2}\right) \quad (1)$$

Where, Φ denotes the QY. The subscripts *x* and *st* denotes the test and standard, respectively. The relative solvent refractive index is indicated as η and *I* is the slope from the plot of the integrated fluorescence intensity vs. absorbance.

Dox loading and release study

Preparation and characterization of g-CQDs@Dox complex

The *g*-CQDs@Dox complex was prepared as reported earlier with minor modification [3]. Briefly, 1 mL of Dox aqueous solution (500 µg mL^{-1}) was mixed with 1 mL of *g*-CQDs solution (0.15 mg mL^{-1}), and allowed to stir at 25 °C overnight. After that, the unreacted Dox was removed by centrifuging the as-prepared solution at 14,000 rpm for 1 h, respectively. Finally, the obtained solid was dispersed in 2 mL ethanol and dried in a vacuum over. The obtained material was stored at 4 °C until use. UV-Vis spectroscopy (Softmax Pro Molecular Device, California, USA) was used for the

characterization of *g*-CQDs, Dox, and *g*-CQDs@Dox complexes. The dox loading efficiency (DLE) and loading content (DLC) was determined by UV-Vis absorption. The amount of Dox loading and amount of *g*-CQDs@Dox was confirmed by taking the absorbance at 485 nm based on standard calibration curves of both Dox and *g*-CQDs. The Dox loading efficiency was calculated as following:

$$DLE\ (\%) = \frac{Amount\ of\ Dox\ in\ g-CQDs}{Initial\ amount\ of\ Dox} \times 100\% \quad (2)$$

$$DLC\ (\%) = \frac{Amount\ of\ Dox\ in\ g-CQDs}{Initial\ amount\ of\ g-CQDs} \times 100\% \quad (3)$$

Measurement of Dox release

To mimic the physiological pH of tumor cells, a certain amount of *g*-CQDs@Dox complex was dissolved in phosphate buffer (10 mL) with varying pH (7.4, 5.0, and 6.0), and the solution was stirred continuously at 37 °C in dark condition. This represents the physiological pH, endolysosomal pH of tumor cells, and the interstitial fluid of tumor cells. After desired time interval, 1 mL of buffer solution was taken and replaced with fresh buffer (1 mL). Next, the buffer solution was centrifuged at 14,000 rpm for 10 min and the released Dox was quantified via UV-Vis absorbance measurement of the supernatant as mentioned above. Each experiment was replicated thrice (n = 3) and data are represented as mean ± s.d.

***In vitro* and *in vivo* studies**

Evaluation of in vitro antitumor properties

The B16F10 (KCLB No. 80008) and MDA (KCLB No. 80065) cells were incubated with DMEM media for 24 h in a humidified atmosphere containing 5% CO_2 with or without *g*-CQDs (0.01,

0.025, 0.05, 0.1, and 0.15 mg mL^{-1}) and *g*-CQDs@Dox. After 24 h, the cells were washed twice with PBS, and incubated with 10 µL of WST-8 dye for 2 h. The absorbance of the solution was measured using a microplate reader at 450 nm. Similarly, the cytotoxicity of *g*-CQDs@Dox complex was evaluated by WST-8 assay, taking *g*-CQDs as positive control. Likewise, dox (10, 20, 40, 60, 80, and 100 µg mL^{-1}) was also taken for evaluation of cell viability in both B16F10 and HepG2 cells.

For the ROS study, the B16F10 (1×10^4 cells/well) and MDA (1×10^4 cells/well) cells were incubated with *g*-CQDs and g-CQDs@Dox, and incubated for 24 h. Next, the cells were washed with PBS, and treated with a ROS sensitive probe 2',7'-dichlorodihydrofluorescin diacetate (H_2DCF-DA) for 30 min. After that, the cells were washed twice with PBS and fresh culture media was added. The intracellular ROS was observed by an inverted fluorescence microscope (Leica DMi8, Germany). For the fluorescent-activated cell sorting (FACS) analysis, the H_2DCF-DA stained cells were visualized in a flow cytometer (FACSCalibur, BD Biosciences, USA) with appropriate excitation lasers. At least 7500 events were recorded, and the cells were gated through M1 (for positive DCF stained cells). The cells without any treatment were considered as control. The cell cycle distribution analysis and cell migration study was conducted as reported in our previous study [4].

Immunocytochemical staining was performed to observe the cytoskeletal aberration of tumor cells. For this, the B16F10 cells (2.5×10^4 cells/well) were incubated with *g*-CQDs and *g*-CQDs@Dox for 24 h at 37 °C with 5% CO_2. After that, the cells were fixed with 3.7% paraformaldehyde (PFA) for 15 min, permeabilized with 0.1% Triton-X 100 for 10 min, followed by blocking with 0.5% normal goat serum for 1 h. After blocking, the cells were incubated with Alexa Flour 488-conjugated F-actin (Molecular Probes, Thermo Scientific, USA) for 30 min. After

that, the cells were mounted with 20 μL aqueous mounting media containing DAPI and visualized with an inverted fluoresce microscope. To study the focal adhesion proteins, the blocked cells were incubated with mouse anti-Paxillin antibody (1:250, Santa Cruz Biotechnology, USA) for 1 h, followed by incubation with FITC-conjugated secondary antibody (1:200). All the images were taken with appropriate filters and compared with the control groups.

For *in vitro* delivery and bioimaging experiments, the B16F10 cells (2.5×10^4 cells/well) were incubated with Dox and *g*-CQDs@Dox complex for 0.5, 2, and 4 h at 37 °C with 5% CO_2 environment. After desired time period, the cells were washed with PBS, fixed with 3.7% PFA for 15 min. After that, the cells were stained with DAPI (50 μg mL^{-1}) for 5 min. After incubation, the cells were washed with PBS, and visualized by an inverted fluorescence microscope to observed the delivery efficiency of free Dox and *g*-CQDs@Dox complex. The excitation wavelength used for DAPI, Dox, and g-CQDs are 405 nm, 593 nm, and 488 nm, respectively. Moreover, the nuclear targeting efficiency of *g*-CQDs was also evaluated by time-dependent fluorescence imaging in B16F10 cells. All the images were taken with appropriate filters, and analyzed by ImageJ (v1.8, NIH, Bethesda, USA) software.

Two-photon cell imaging

MDA cells were treated with 10.0 μg mL^{-1} *g*-CQDs for 1 h, washed with pH 7.4 PBS two times and fixed with 4% formaldehyde prior to imaging. Fluorescent two-photon images were obtained using Leica TCS SP5 II Advanced System and a 25× objective lens (obj. HCX PL APO 25× / 1.10 W CORR CS, Leica, Germany). The two-photon excitation wavelength was tuned to 800 nm. Emission light was collected in three channels. 400–480 nm (blue), 490–570 nm (green) and 580–660 nm

(yellow). Acquired images were processed using LAS AF Lite (Leica, Germany). The image intensity was calculated using Image Pro 6.0.

Hemocompatibility assay

For biosafety analysis, the blood biocompatibility test was performed using the *g*-CQDs and *g*-CQDs@Dox, respectively. For this, freshly collected red blood cells (RBCs, 6×) were incubated with DW (2 mL), PBS buffer (2 mL), *g*-CQDs (2 mL), and *g*-CQDs@Dox (2 mL) for 120 min at 37 °C. After that, the blood was centrifuged at 3,400 rpm for 10 min, and 100 µL supernatant was collected for spectrophotometric analysis. The absorbance was recorded at 540 nm (as a function of hemoglobin) and the % of hemolysis was calculated as following:

$$\%\ of\ hemolysis = \frac{Ab_t - Ab_{nc}}{Ab_{pc} - Ab_{nc}} \times 100 \quad (4)$$

Where, Ab_t, Ab_{nc}, and Ab_{pc} indicate the absorbance of treated samples, negative control, and positive control, respectively.

Pharmacokinetics and biodistribution study

The pharmacokinetics and biodistribution study, the *g*-CQDs@Dox was directly used due to the auto-fluorescence ($\lambda^{ex}/_{em}$ of *g*-CQDs = $^{350}/_{516}$ nm) property of the nanocarrier. The female Balb/c nude mice (4-6 week old) were used in this study. All the mice were given free access food and water. For pharmacokinetic study, 100 µL of *g*-CQDs@Dox was injected through tail vein (*n* = 3), and the blood (10 µL) was collected in every 2-3 h intervals. Each blood sample was washed with PBS, lysed with lysis buffer (eBioscience, Thermo-Fischer Scientific, USA), and the

concentration of the *g*-CQDs@Dox was measured by using a fluorimeter (Fluoromax 4, Horiba Jobin, France). The standard curve was prepared using serial dilution of the material. Blank samples (without nanocarrier) without injection was also analyzed to reduce background fluorescence of the test samples. The pharmacokinetic parameters, such as half-life ($t_{1/2}$), relative volume (V), and area under curve (AUC) were calculated as reported earlier [5]. Likewise, the accumulation of *g*-CQDs@Dox in the tumor site was also examined as described above.

For *ex vivo* biodistribution analysis, the g-CQDs@Dox was administrated to mice by intravenous injection. The mice were sacrificed, and organs were harvested (n = 3) at predetermined time points 1h, 3h, 6h, 12h and 24h. Fluorescence image of harvested organs measured using in vivo imaging system (IVIS Spectrum, Perkin Elmer, USA) and organs were homogenized for quantitative analysis. Fluorescence of each organ used to analyze the g-CQDs@Dox accumulation.

In vivo antitumor tests

The subcutaneous melanoma tumor model was established by injecting 100 µL of B16F10 cells (2×10^5 cells in PBS) on the right flank of Balb/c nude mice. The study was conducted in four group ($N = 4$), the PBS group ($n = 3$), the Dox group ($n = 3$), *g*-CQDs group ($n = 3$), *g*-CQDs@Dox group (n = 5), respectively. Each mouse received a total of seven intratumoral injections every second day with various formulations. The Dox group received a dose of 2 mg/kg and *g*-CQDs@Dox group received a dose of 2 mg kg^{-1}, respectively. The PBS-treated and Dox-treated groups were taken as negative and positive controls. The tumor volume was calculated as following:

Tumor volume (V) = Tumor length (L) × width (W^2) × 0.5 (5)

After 25 days of treatment, the mouse was euthanized, and the tumor tissues were harvested, formalin-fixed, paraffin-embedded, and stained with hematoxylin and eosin (H&E) for histopathological examination. At the same time, the mouse blood was collected to examine the biosafety of the various formulations.

Statistical analysis

All the data were presented as mean ± s.d. of triplicate ($n = 3$) experiments. Statistical significance between control and treated groups were analyzed through One-way ANOVA (Origin Pro v9.0, Origin Labs, USA) and student *t*-test and a value of $^{*}p < 0.05$ was considered to be statistically significant.

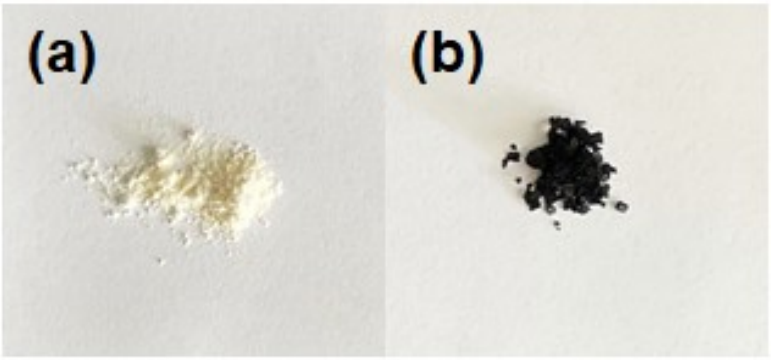

Fig. S1. Digital photograph of the **(a)** Phloroglucinol, and **(b)** *g*-CQDs.

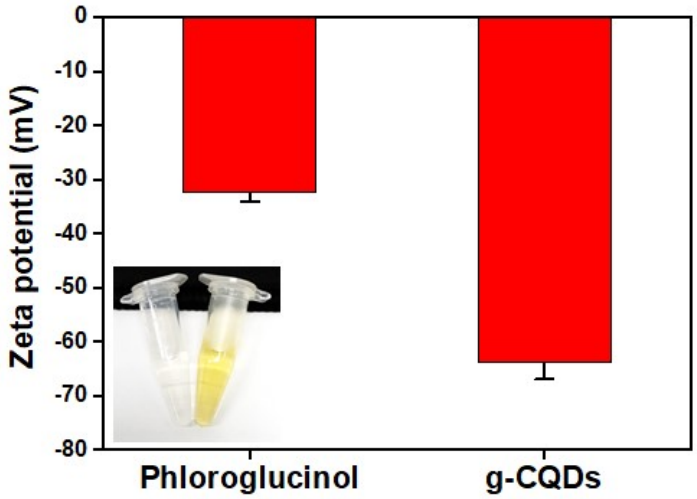

Fig. S2. The zeta potential (ζ) of the phloroglucinol and *g*-CQDs (inset: ethanol dispersed phloroglucinol and *g*-CQDs used for the study).

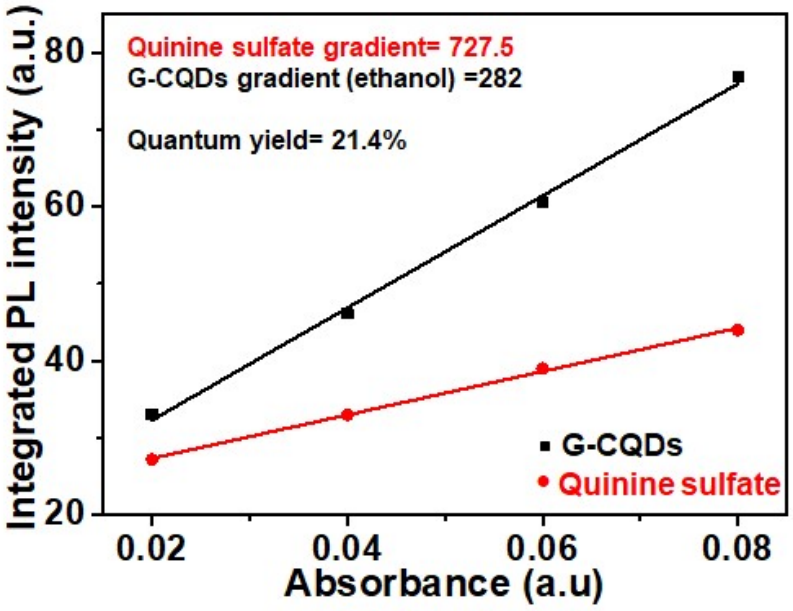

Fig. S4. The quantum yield (QY) of the ethanol dispersed *g*-CQDs (Quinine sulfate was taken as the reference value).

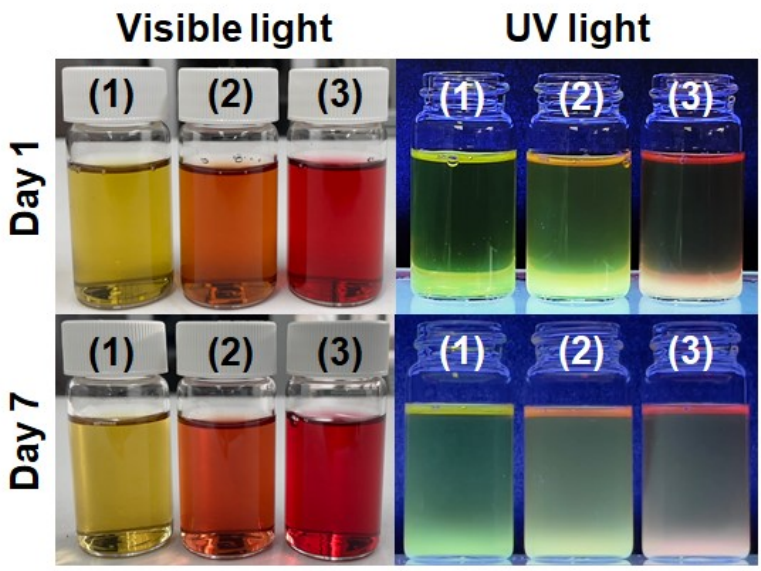

Fig. S4. Stability of *g*-CQDs up to 7 days in (1) PBS, (2) FBS, and (3) DMEM media under visible light and UV light.

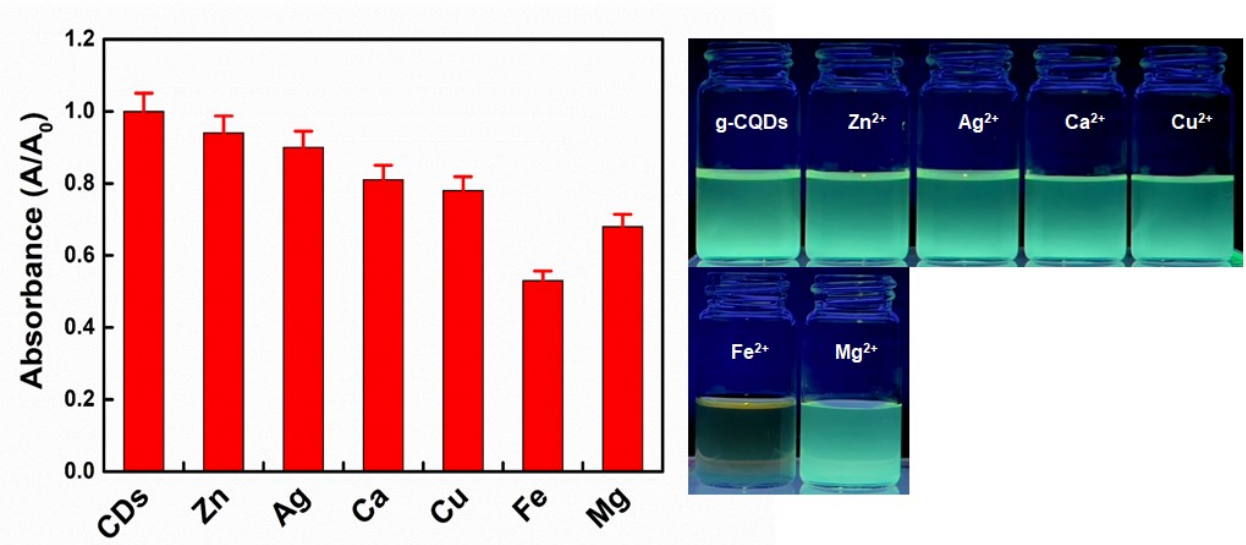

Fig. S5. The UV-Vis absorbance spectra (A/A_0) of the *g*-CQDs in the presence of Zn^{2+}, Ag^{2+}, Ca^{2+}, Cu^{2+}, Fe^{2+}, and Mg^{2+} (100 μM) with corresponding images under 365 nm UV light.

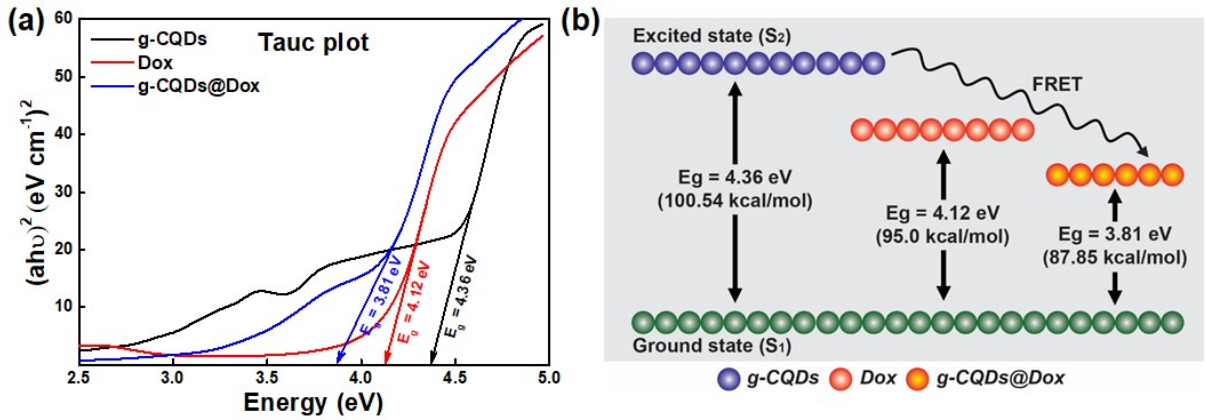

Fig. S6. (a) Tauc plot of *g*-CQDs, Dox, and *g*-CQDs@Dox showing the band gap intensities (values are in eV) derived from the corresponding UV-Vis spectra. **(b)** Schematic illustration for the FRET mechanism of *g*-CQDs and Dox conjugation.

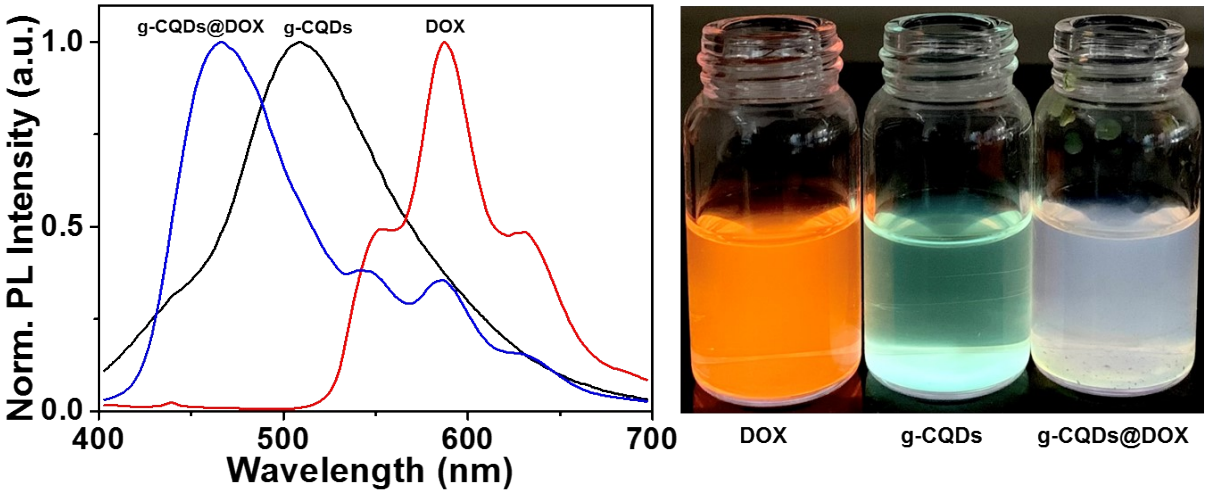

Fig. S7. (a) The PL emission spectra of *g*-CQDs, free Dox, and *g*-CQDs@Dox complex. **(b)** The PL spectra for all the sample was recorded at 350 nm excitation.

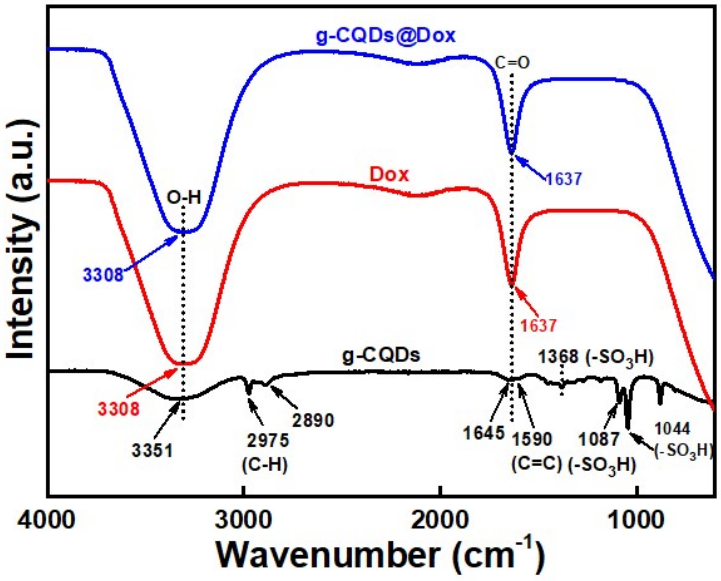

Fig. S8. The FT-IR spectra of pure *g*-CQDs, free Dox, and *g*-CQDs@Dox complex.

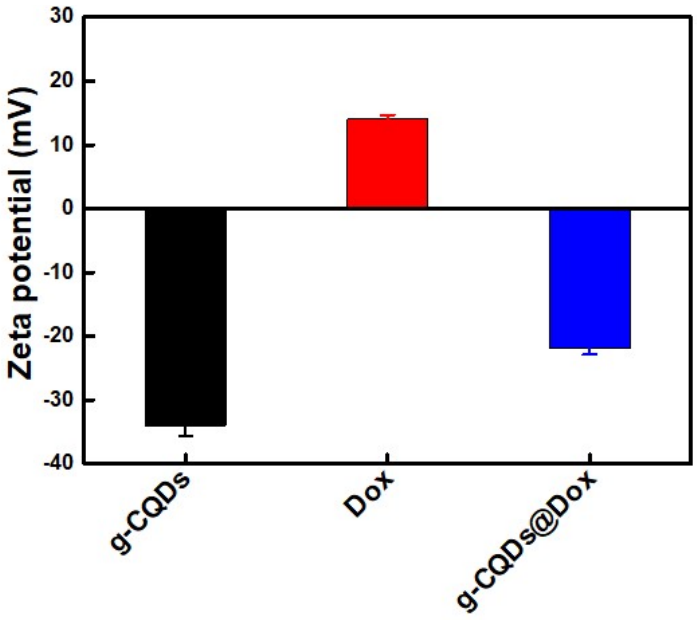

Fig. S9. The zeta potential (ζ) of the as-prepared *g*-CQDs, free Dox, and *g*-CQDs@Dox.

Fig. S10. The effect of solvent pH on dispersion property of *g*-CQDs.

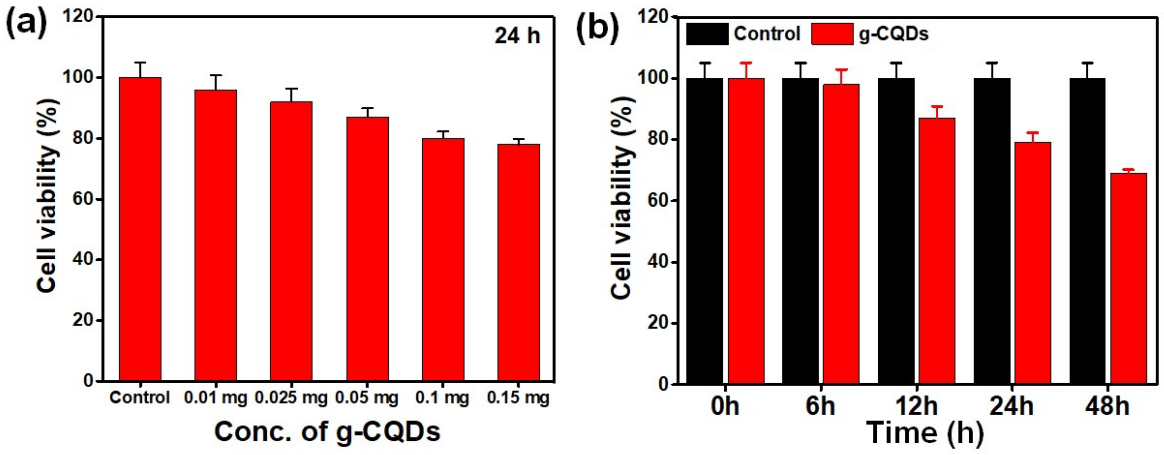

Fig. S11. (a) Concentration-dependent (0, 0.01, 0.025, 0.05, 0.1, and 0.15 mg mL^{-1}, 24 h) and **(b)** Time-dependent (0.15 mg mL^{-1}, 0-48 h) cytotoxicity of *g*-CQDs against B16F10 cells. Data are mean ± s.d. (n = 3), statistical significance at $^{*}p < 0.05$.

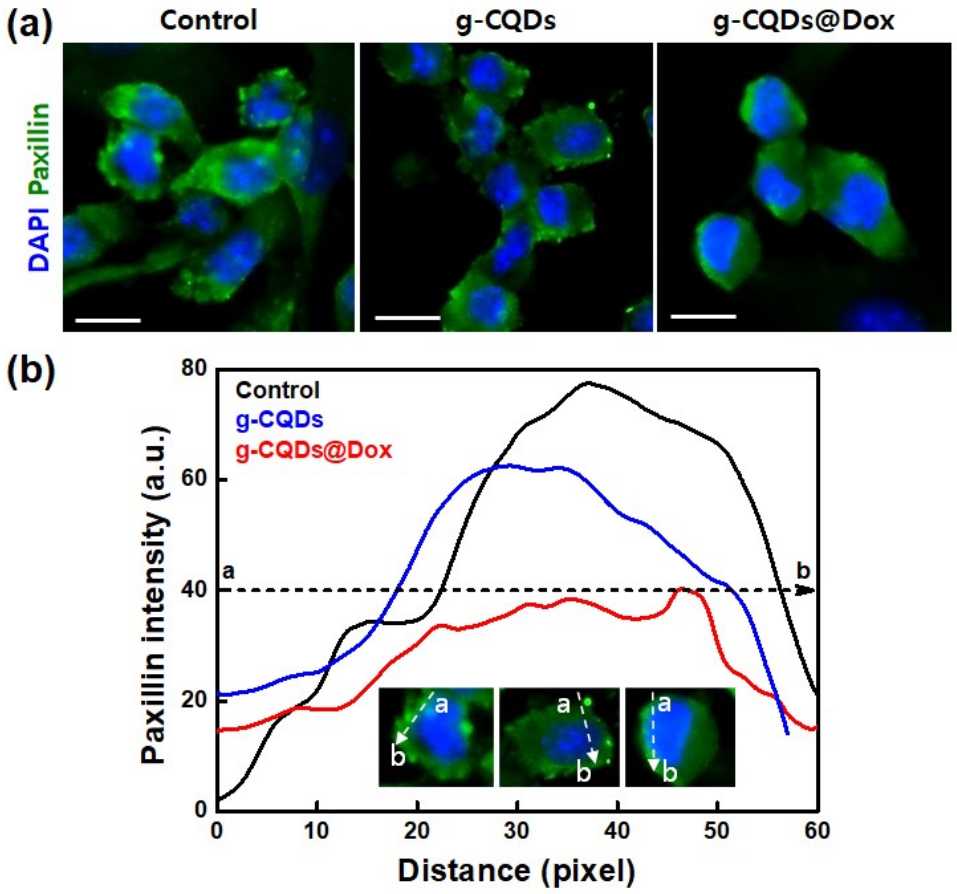

Fig. S12. (a) Immunofluorescence staining of B16F10 cells showing the expression of Paxillin following *g*-CQDs and *g*-CQDs@Dox treatment for 24 h. Scale bar: 100 μm. **(b)** Representative line-scan intensity profile of Paxillin.

Colocalization study:

For this, MDA cells (2×10^4 cells/well) were cultured in DMEM with 5% CO2 at 37 °C for 24 h. Before imaging, the cells were incubated with 10.0 µg mL^{-1} *g*-CQDs for 1 h. After that, the cells were incubated with 100 µM Dil C-18, Sigma-Aldrich, USA (dissolved in 1% DMSO) for 10 min at 37 °C. Next, the cells were washed twice with warm PBS, fixed with 3.7% paraformaldehyde, and mounted with appropriate mounting media. After that, the cells were visualized with an inverted laser confocal microscope (63× obj., Zeiss, Germany) with excitation laser 488 nm and 532 nm, respectively. The captured imaged were analyzed with ZEN software (v2.1, Zeiss, Germany), and the Colocalization experiment was conducted using ImageJ software with Fiji plugins (plugin Info. Coloc analyzer). The Ch1(Red)/Ch2(Green) volume = 1.05%, R<threshold = 0.019, R_{coloc} = 0.597, and % of Colocalization = 18.14%, respectively.

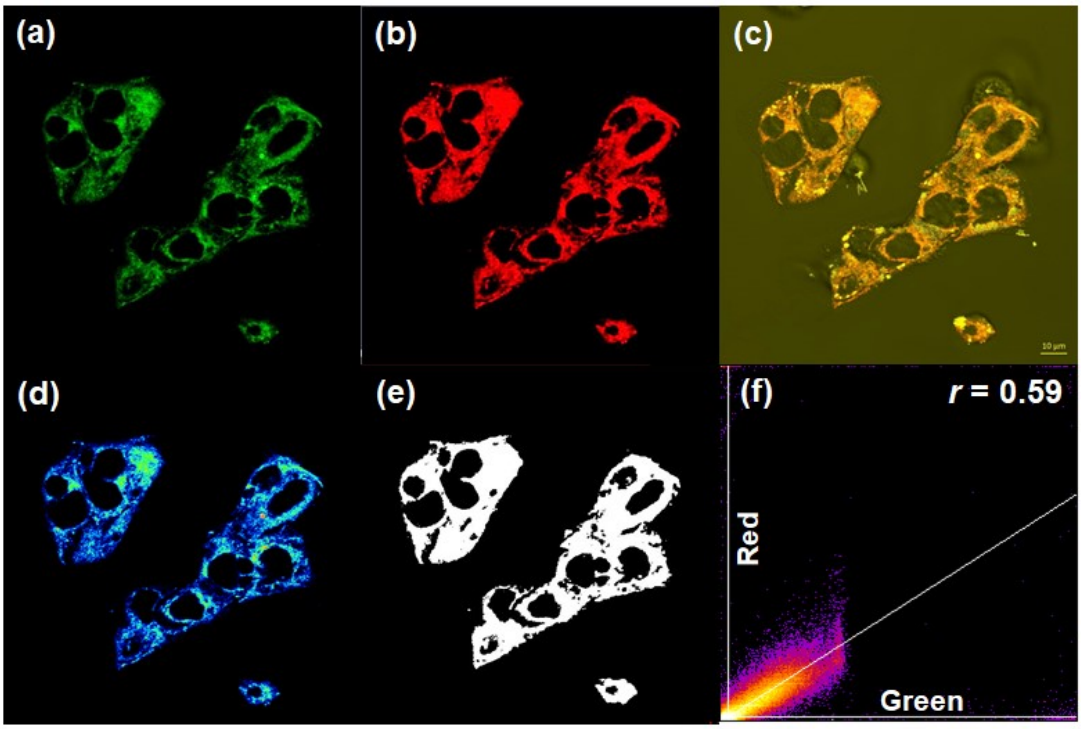

Fig. S13. Colocalization experiment for the membrane-targeting property of *g*-CQDs in MDA cells. Representative CLSM images of MDA cells stained with **(a)** g-CQDs (green), **(b)** Dil (red), **(c)** merge image, **(d)** pseudocolor merge image, **(e)** Colocalization pixel map, and **(f)** Pearson coefficient (R_{coloc} = R_{total} of Red/Green fluorescence = 0.570), respectively. Scale bar: 10 µm.

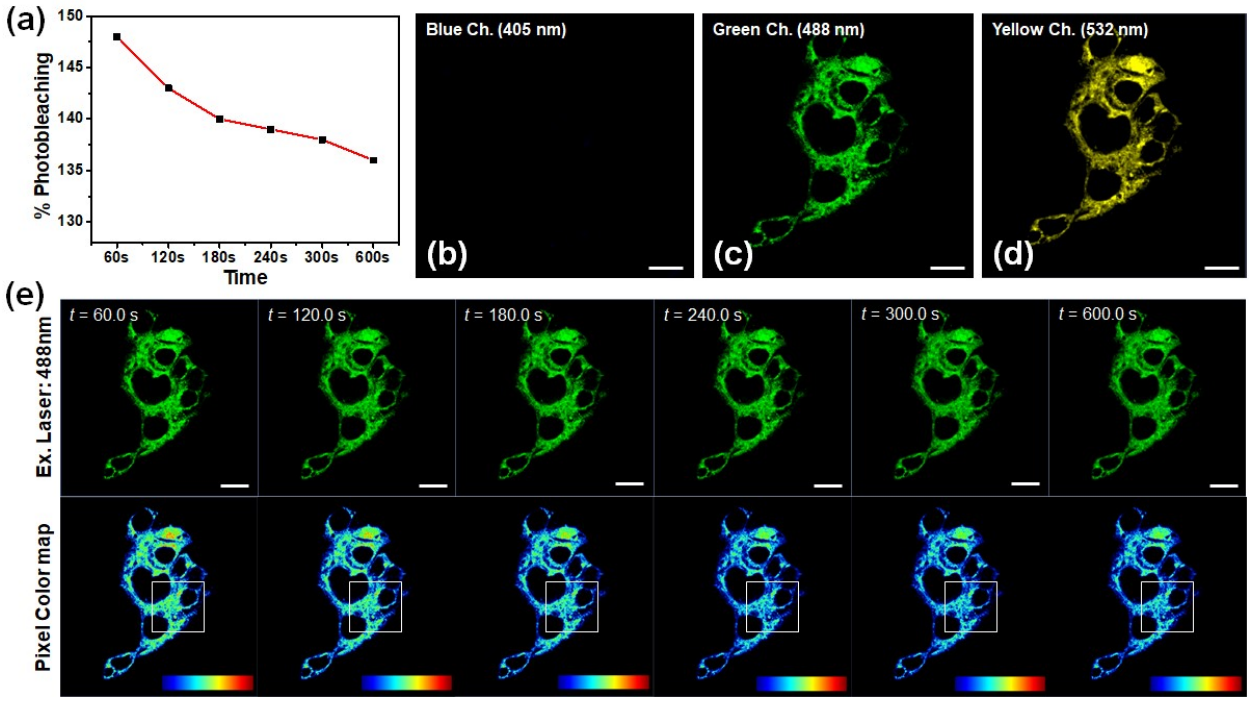

Fig. S14. Photobleaching and long-term stability of *g*-CQDs. **(a)** Photobleaching percentage of g-CQDs from MDA cells after 1 h of incubation. **(b-d)** CLSM images of MDA cells stained with g-CQDs at different excitation lasers. **(e)** Time-dependent CLSM images of MDA cells exposed to 488 nm laser for 60-600 s with corresponding pixel color map indicating the bleached intensity. Scale bar: 10 µm.

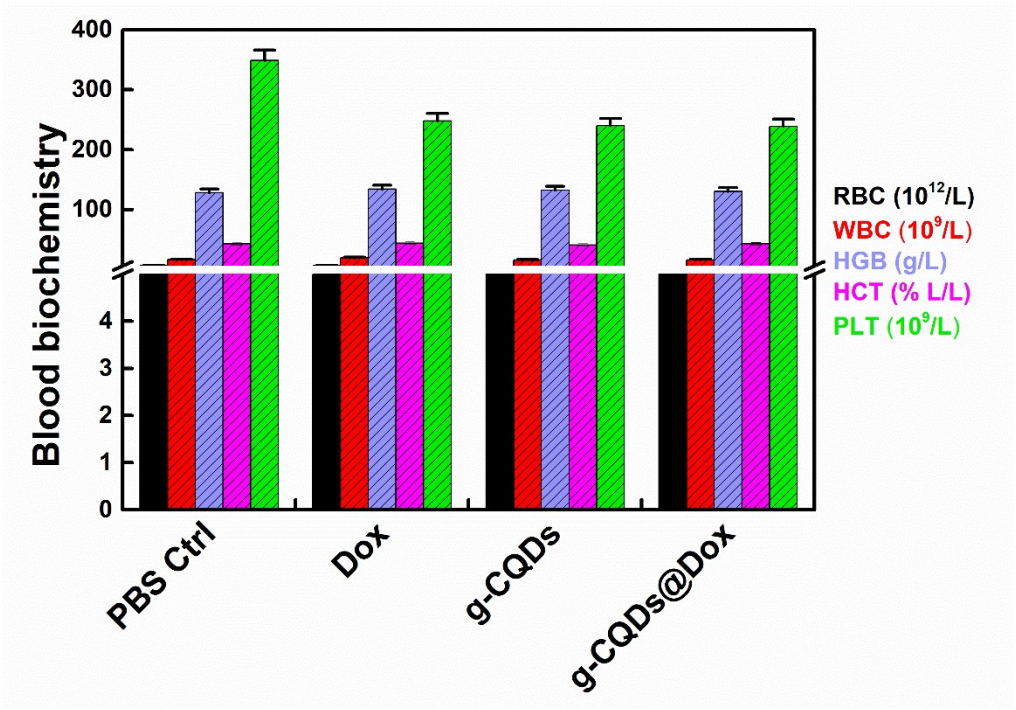

Fig. S15. Complete blood count (CBC) of the tumor-bearing Balb/C nude mice after 25 days of therapy. Data are mean ± s.d. (n = 3), statistical significance at $^{*}p < 0.05$.

References:

1. F. Yuan, T. Yuan, L. Sui, Z. Wang, Z. Xi, Y. Li, X. Li, L. Fan, Z. a. Tan and A. Chen, *Nature communications*, 2018, **9**, 1-11.
2. M. Moniruzzaman and J. Kim, *Applied Surface Science*, 2021, **552**, 149372.
3. R. Wu, J. Liu, D. Chen and J. Pan, *ACS Applied Nano Materials*, 2019, **2**, 4333-4341.
4. S. D. Dutta, T. Park, K. Ganguly, D. K. Patel, J. Bin, M.-C. Kim and K.-T. Lim, *ACS Applied Bio Materials*, 2021, **4**, 6853-6864.
5. J. Shao, H. Xie, H. Huang, Z. Li, Z. Sun, Y. Xu, Q. Xiao, X.-F. Yu, Y. Zhao and H. Zhang, *Nature communications*, 2016, **7**, 1-13.